Stem Cell Reports
Article

ISSCR

OPEN ACCESS

Tropomyosin 1 deficiency facilitates cell state transitions and enhances hemogenic endothelial cell specification during hematopoiesis

Madison B. Wilken,[1,8] Gennadiy Fonar,[1,8] Rong Qiu,[1] Laura Bennett,[2] Joanna Tober,[2] Catriana Nations,[3,4] Giulia Pavani,[3,4] Victor Tsao,[1,5] James Garifallou,[1] Chayanne Petit,[1] Jean Ann Maguire,[3] Alyssa Gagne,[3] Nkemdilim Okoli,[1,5] Paul Gadue,[3,4] Stella T. Chou,[6,7] Deborah L. French,[3,4] Nancy A. Speck,[2] and Christopher S. Thom[1,7,9,*]

[1]Division of Neonatology, Children's Hospital of Philadelphia, Philadelphia, PA, USA
[2]Department of Cell and Developmental Biology, Perelman School of Medicine, University of Pennsylvania, Philadelphia, PA, USA
[3]Center for Cellular and Molecular Therapeutics, Children's Hospital of Philadelphia, Philadelphia, PA, USA
[4]Department of Pathology and Laboratory Medicine, Children's Hospital of Philadelphia, Philadelphia, PA, USA
[5]School of Arts and Sciences, University of Pennsylvania, Philadelphia, PA, USA
[6]Division of Hematology, Children's Hospital of Philadelphia, Philadelphia, PA, USA
[7]Department of Pediatrics, Perelman School of Medicine, University of Pennsylvania, Philadelphia, PA, USA
[8]These authors contributed equally
[9]Lead contact
*Correspondence: thomc@chop.edu
https://doi.org/10.1016/j.stemcr.2024.08.001

SUMMARY

Tropomyosins coat actin filaments to impact actin-related signaling and cell morphogenesis. Genome-wide association studies have linked *Tropomyosin 1* (*TPM1*) with human blood trait variation. *TPM1* has been shown to regulate blood cell formation *in vitro*, but it remains unclear how or when *TPM1* affects hematopoiesis. Using gene-edited induced pluripotent stem cell (iPSC) model systems, we found that *TPM1* knockout augmented developmental cell state transitions and key signaling pathways, including tumor necrosis factor alpha (TNF-α) signaling, to promote hemogenic endothelial (HE) cell specification and hematopoietic progenitor cell (HPC) production. Single-cell analyses revealed decreased *TPM1* expression during human HE specification, suggesting that *TPM1* regulated *in vivo* hematopoiesis via similar mechanisms. Analyses of a *TPM1* gene trap mouse model showed that *TPM1* deficiency enhanced HE formation during embryogenesis, without increasing the number of hematopoietic stem cells. These findings illuminate novel effects of *TPM1* on developmental hematopoiesis.

INTRODUCTION

Tropomyosin 1 (*TPM1*) is one of four mammalian *Tropomyosin* genes (*TPM1-4*) that bind virtually all cellular actin to regulate cell shape, strength, and molecular signaling (Gateva et al., 2017; Meiring et al., 2018). *TPM* genes produce >40 protein isoforms, each of which can differentially impact actin filament structure and cellular dynamics (Gateva et al., 2017; Schevzov et al., 2011). For example, some high-molecular-weight *TPM1* isoforms (e.g., 1.6/1.7) associate with actin stress fibers that typically promote cell adhesion (Gateva et al., 2017), whereas low-molecular-weight *TPM1* isoforms (e.g., 1.8/1.9) promote lamellipodial persistence and cell motility (Brayford et al., 2016). TPM1 activities are known to impact neuronal, cardiac, and ocular tissue development (Gunning and Hardeman, 2017; Kubo et al., 2013; Shibata et al., 2021). Genome-wide association studies (GWASs) have implicated *TPM1*-associated polymorphisms with human blood trait variation (Chen et al., 2020; Thom et al., 2020a; Vuckovic et al., 2020), suggesting that *TPM1* may also regulate blood cell formation and/or function.

Hematopoiesis is a highly orchestrated process by which embryonic endothelial cells develop into specialized "hemogenic" endothelial (HE) cells. HE cells produce hematopoietic stem and progenitor cells that support mature blood cell formation throughout the mammalian lifespan (Dzierzak and Speck, 2008). Hematopoietic stem cells (HSCs) can repopulate bone marrow in transplantation experiments and give rise to hematopoietic progenitor cells (HPCs). HPCs are immature cells that self-renew and differentiate into mature blood cell lineages. We will refer to progenitor populations as HPCs as a more inclusive term in this manuscript, except for transplantation experiments that explicitly test HSC function. The first HPCs are produced in the embryonic yolk sac during primitive hematopoiesis. Later, HPCs are produced in several locations, including the dorsal aorta-gonad-mesonephros (AGM) region during definitive hematopoiesis. Definitive HE specification occurs at the onset of cardiac function and pulsatile blood flow in the embryo (Lucitti et al., 2007). Recent findings have discriminated multiple waves of definitive hematopoiesis in the AGM, including production of short-lived multipotent progenitor cells from murine embryonic day (E)9.5–E10.5 post-conception that precedes generation of transplantable HSCs around E11.5 (Dignum et al., 2021).

While the stages of hematopoietic development are well characterized, an inability to efficiently recapitulate

primitive or definitive blood formation *in vitro* demonstrates that some factors remain unknown. Factors that regulate definitive HE specification include coordinated retinoic acid, cKit, and Notch pathway signaling, as well as tight cell-cycle control (Goldie et al., 2008; Gritz and Hirschi, 2016; Marcelo et al., 2013). Meis1 activity also helps to establish HE identity (Coulombe et al., 2023), as do proinflammatory signals from tumor necrosis factor alpha (TNF-α) that activate Notch and nuclear factor κB (NF-κB) signaling pathways to establish HPC fate (Espín-Palazón et al., 2014). HE cells are marked by expression of RUNX1, which cooperates with transforming growth factor β (TGF-β) signaling to regulate HPC formation (Howell et al., 2021). During both primitive and definitive hematopoiesis, coordinated transcriptional, signaling, and structural changes establish hematopoietic identity and prepare HE cells to undergo a dramatic morphogenesis from planar, adherent cell types into spherical, non-adherent HPCs. This cell state change from HE to HPC is termed the endothelial-to-hematopoietic transition (EHT) (Kissa and Herbomel, 2010; Ottersbach, 2019). HE cell specification and EHT can be monitored using *in vitro* cell culture systems that model hematopoiesis (Eilken et al., 2009).

Following endothelial formation and HE cell specification from mesodermal origins, EHT resembles an epithelial-to-mesenchymal cell state transition (EMT) (Howell et al., 2021). Tropomyosins are known to regulate cell state transitions, including EMTs, in several tissue and physiologic states (Kalluri and Weinberg, 2009). Increased *TPM1* expression has been observed in cells undergoing EMT in the murine eye lens epithelium (Kubo et al., 2013), and concurrent *TPM1* and *TPM2* deletion inhibited normal eye lens formation (Shibata et al., 2021). *TPM1* deficiency has also been linked with EMT during cancer progression, as well as increased proliferation and migration in cell lines designed to mimic solid tumor models (Bakin et al., 2004, 2005; Dai and Gao, 2021; Pan et al., 2017; Wang et al., 2019). For example, *TPM1* mediates TGF-β-induced migratory behavior via actin cytoskeletal rearrangements and stress fiber formation in cultured epithelial cells (Bakin et al., 2004). *TPM1* also constrains TNF-α-mediated inflammatory signaling to regulate arterial endothelial actin organization, migration, and proliferation (Gagat et al., 2021). Actin cytoskeletal dynamics (Lancino et al., 2018), TGF-β (Howell et al., 2021; Ottersbach, 2019), and TNF-α signaling (Espín-Palazón et al., 2014) also impact hematopoiesis, suggesting that *TPM1* might regulate blood formation through similar mechanisms.

Our previous work, using genetically modified induced pluripotent stem cell (iPSC) lines, showed that *TPM1* constrained *in vitro* primitive hematopoiesis by limiting HPC formation (Thom et al., 2020a). In the current study, we wanted to examine the mechanisms and developmental stages through which *TPM1* impacted hematopoiesis in order to elucidate novel approaches to enhance *in vitro* blood formation and contribute to a broader understanding of the role tropomyosins play in regulating cell development. We hypothesized that *TPM1* may regulate HE cell specification and/or EHT during primitive and/or definitive hematopoiesis, given the established links between *TPM1* and cell state transitions in other developmental systems. We found that *TPM1* expression was downregulated during hematopoiesis at the HE cell and HPC stages *in vitro* and *in vivo*. In assays of cultured iPSCs, constitutive *TPM1* deficiency promoted primitive HE cell formation without compromising HPC function. The increase in HE cells was accompanied by changes in signaling pathways known to regulate HE cell formation and function, including epistatic interactions with TNF-α signaling. Murine studies confirmed our *in vitro* findings that *TPM1* haploinsufficiency increased definitive HE cell specification *in vivo*, although these effects were limited to E9.5–E10.5 HE and progenitor cell production without increasing transplantable HSC production. These findings define a novel role for *TPM1* in hematopoiesis across mammalian species and developmental ontogeny.

RESULTS

TPM1 deficiency enhances *in vitro* endothelial cell formation without augmenting cell-cycle kinetics

An iPSC model system was used to study the role of *TPM1* during *in vitro* primitive hematopoiesis, which includes defined iPSC, mesoderm, endothelial, and HPC stages of development (Thom et al., 2020a) (Figure 1A). Our first goal was to analyze TPM1 protein expression at these developmental stages. Consistent with our prior findings, high-molecular-weight TPM1 protein (e.g., TPM1.6/1.7) was expressed in adherent cell types, including undifferentiated iPSCs as well as iPSC-derived mesoderm and endothelial cells, and was abolished in non-adherent HPCs (Figure 1B). The absence of high-molecular-weight TPM1 protein was contrasted by the presence of low-molecular-weight TPM1 isoforms (e.g., TPM1.8/TPM1.9) in HPCs and mature blood cell types (Figures S1A and S1B). These dynamic changes in expression suggest that high-molecular-weight TPM1 might impact adherent cell biology or development, including endothelial cells.

Analysis of developmental kinetics and cell surface marker expression showed that cultured *TPM1* knockout (KO) iPSCs that lacked expression of all *TPM1* isoforms had increased endothelial cell and HPC yields compared with isogenic wild-type (WT) controls (Wilken et al., 2023) (Figures 1C–1E and S1C). These findings, using a recently derived iPSC line (Wilken et al., 2023), were

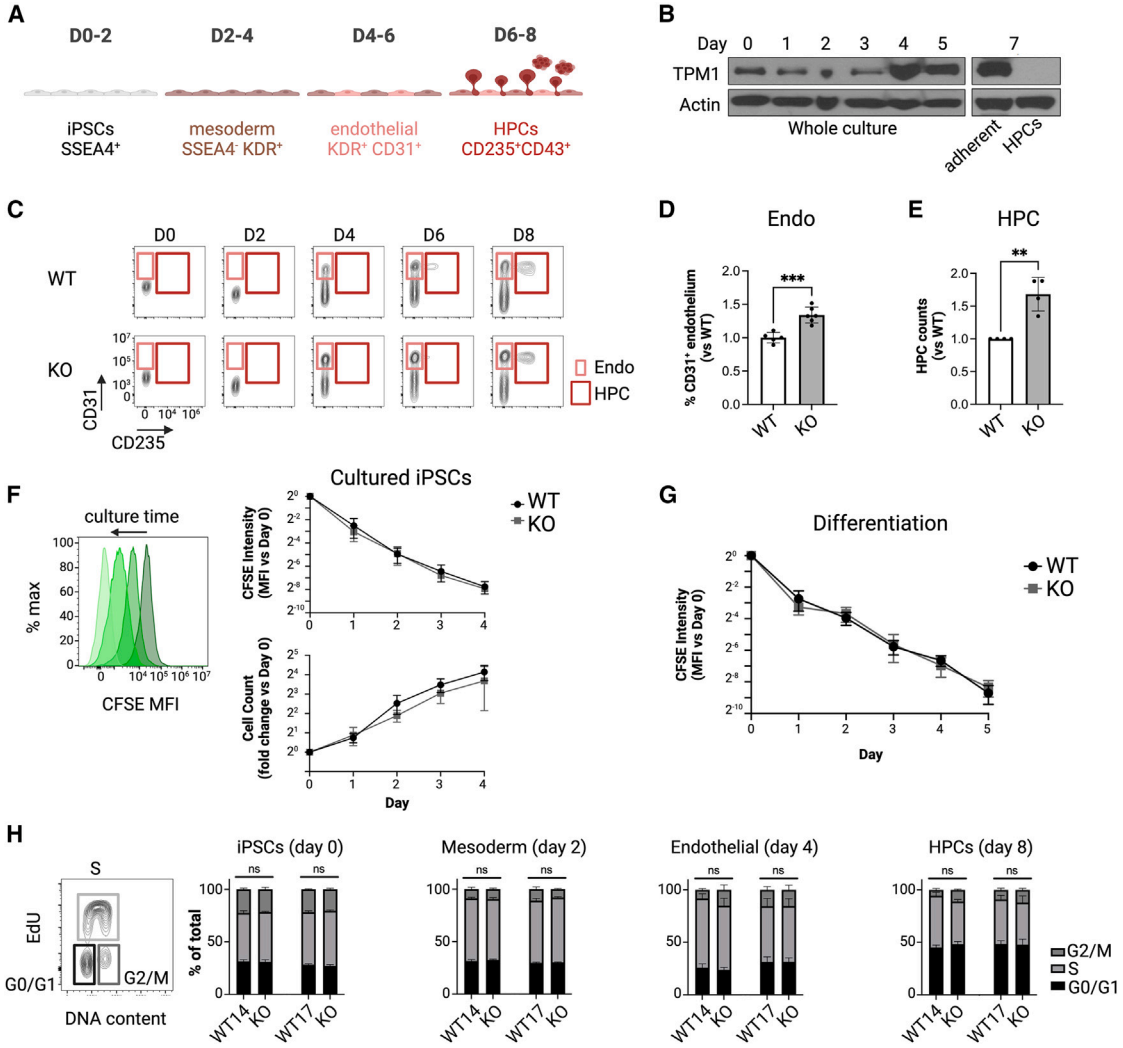

Figure 1. *TPM1* deficiency enhances *in vitro* endothelial and hematopoietic progenitor cell formation without enhancing proliferation

(A) Schematic overview of primitive *in vitro* hematopoiesis, including relevant cell types and cell surface markers over the differentiation timeline.

(B) Western blot showing TPM1.6/1.7 protein expression over the course of *in vitro* hematopoiesis. On day 7, adherent cells (mesoderm, endothelial, stromal) and non-adherent HPCs were collected and analyzed separately.

(C) Exemplary flow cytometry plots during differentiation, with boxes highlighting CD31$^+$ endothelial cells and CD235$^+$ HPCs in wild-type (WT) and *TPM1KO* (KO) cultures.

(D) *TPM1KO* cultures show enhanced CD31$^+$ endothelial cell percentage (%) vs. isogenic WT cultures on days 4–6 (CHOP17 cell lines). Bar plots show mean ± SD, significance assessed by t test (n = 5–6 cultures in 3 experiments).

(E) *TPM1KO* cultures produce more non-adherent CD235$^+$ HPCs on day 7–8 than isogenic WT controls (CHOP17). Bar plots show mean ± SD (n = 4 experiments).

(F) Mean fluorescence intensity (MFI) for CFSE, a non-toxic cell permeable dye, diminishes with each cell division in culture. CFSE MFI diminishes identically in cultured isogenic WT and *TPM1KO* iPSCs (CHOP10). Similarly, there were no significant differences in WT vs. *TPM1KO* cell expansion over time by direct cell counting (n = 3 experiments).

(G) CFSE MFI diminishes identically in isogenic WT and *TPM1KO* cells undergoing primitive hematopoietic differentiation (CHOP10, n = 4 experiments).

(H) EdU-based analysis allows identification of cells in G0/G1, S, and G2/M cell-cycle stages. Analysis of *TPM1KO* cells at the iPSC, day 2 SSEA4$^-$ (mesoderm), day 4 CD31$^+$ (endothelial), and day 8 CD235$^+$ non-adherent HPC stages showed no significant differences in cell-cycle progression compared with isogenic WT controls (n = 4–9 per group). Bar plots show mean ± SEM. *p < 0.05, **p < 0.01, ****p < 0.0001 by ANOVA.

consistent with prior results in two iPSC lines of different genetic backgrounds (Thom et al., 2020a). These three iPSC lines were used interchangeably throughout the study.

We reasoned that *TPM1KO* could increase endothelial and HPC production by enhancing proliferation (Canu et al., 2020) or by enhancing HE cell specification (Kalluri and Weinberg, 2009; Ottersbach, 2019). To determine if *TPM1KO* altered cell proliferation, we analyzed the mean fluorescence intensity (MFI) of the cell-permeable carboxyfluorescein succinimidyl ester (CFSE) dye over time (Figure 1F). CFSE staining decreased identically in *TPM1KO* and isogenic WT control lines, confirming that *TPM1KO* cells proliferated normally during differentiation (Figures 1F, 1G, and S1D–S1F). To determine if cell-cycle progression was altered at specific developmental stages, relevant cell populations were stained with 5-ethynyl-2′-deoxyuridine (EdU). *TPM1KO* cell-cycle kinetics did not significantly differ from isogenic controls at any analyzed stage (Figures 1H and S1G). Thus, mechanisms other than increased cell proliferation must have been responsible for increased endothelial and hematopoietic cell production in cultured *TPM1KO* cells.

Increased expression of HE-related genes and signaling pathways in *TPM1KO* lines

To detect transcriptional evidence of developmental perturbations in cultured *TPM1KO* cells, bulk RNA sequencing analysis was performed on cells at defined stages of hematopoietic differentiation Chen et al., 2013; Kuleshov et al., 2016; Kucukural et al., 2019; Xie et al., 2021) (experimental procedures). Clustering analyses showed that *TPM1KO* gene expression generally matched isogenic WT controls at each stage of differentiation (Figures 2A and S2A). This occurred despite changes in actin- and focal adhesion-related gene expression in most *TPM1KO* cell types (Figure 2B; Table S1). These findings supported the notion that *TPM1KO* cultures generally underwent normal developmental stage progression, albeit with expected differences in actin regulatory processes.

In assessing HE-related gene expression, we noted increased EMT-related gene expression in *TPM1KO* cells at the endothelial stage by gene set enrichment analysis (Figure 2C; Table S2). We also observed increased *cKIT* gene expression, which is important for HE specification (Marcelo et al., 2013), in *TPM1KO* endothelial cells (Figure 2D). No significant changes in blood or hematopoietic-related gene expression pathways were identified at day 4 of differentiation, which preceded full induction of *RUNX1* and the downstream hematopoietic program (Figure 2D). These observations suggested that *TPM1KO* enhanced HE cell specification to increase endothelial cell and HPC yields.

We envisioned two non-mutually exclusive mechanisms by which *TPM1KO* and actin cytoskeletal perturbations could enhance HE cell specification and HPC yield. First, *TPM1KO* may promote HE cells to "escape" from the adherent endothelial cell environment to form HPCs via a biophysical mechanism (Ottersbach, 2019), as supported by the altered expression of genes impacting extracellular matrix-receptor interactions and cell migration (Figure 2E; Table S1). Second, altered actin dynamics could change the scaffolding necessary for signaling pathway regulation, including pathways necessary for HE cell specification and HPC formation (Colin et al., 2016). Altered KRAS and Rap1 GTPase signaling changes were noted in *TPM1KO* cultures at the mesoderm stage and continued through differentiation (Figure 2F; Table S1). Additional changes in TNF-α signaling via NF-κB were evident in *TPM1KO* cells, particularly at the endothelial stage, along with modest alteration in TGF-β signaling (Figure 2F; Table S2). TGF-β (Howell et al., 2021), TNF-α (Espín-Palazón et al., 2014), and GTPase signaling mechanisms (Saxena et al., 2016) can each promote HE cell specification and/or EHT. Taken together, these findings suggested that *TPM1KO* increased HE specification through multiple mechanisms, including altering actin dynamics, physical cell interactions, and signaling activities in developing endothelial cells.

The link between *TPM1* and TNF-α signaling was intriguing, considering recent data linking tropomyosin-mediated actin regulation to inflammatory signaling modulation (Gagat et al., 2021; Li et al., 2022). To functionally interrogate our RNA sequencing findings, we modulated TNF-α signaling during endothelial specification and HPC formation in WT and *TPM1KO* cultures using a small-molecule inhibitor that stabilizes the trimeric TNF-α receptor complex in an abnormal position (O'Connell et al., 2019). We identified epistatic effects of TNF-α inhibition on *TPM1KO* cultures, with HPC output reduced to WT levels (Figure S2B). Paradoxically, low-dose inhibitor treatment (10 μM) enhanced HPC production in both WT and *TPM1KO* contexts, perhaps through mild receptor stimulation as seen with other TNF receptor antagonists (Chen and Oppenheim, 2016). Direct addition of recombinant TNF-α during endothelial specification augmented WT HPC production to the level of *TPM1KO* cultures, without significantly altering *TPM1KO* HPC output (Figure S2C).

TPM1 deficiency enhances HE specification to produce functional HPCs

To functionally determine the effect of *TPM1KO* on HE cell specification, sorted day 4–5 $CD31^{+}CD43^{-}$ endothelial cells were plated in limiting dilution and cultured in hematopoietic cytokines, and $CD43^{+}$ HPCs were quantified (Howell et al., 2021) (Figure 3A). These experiments demonstrated an increased frequency of HE cells in *TPM1KO* cultures in two independent iPSC lines (Figure 3B). Since robust cell surface markers for primitive HE

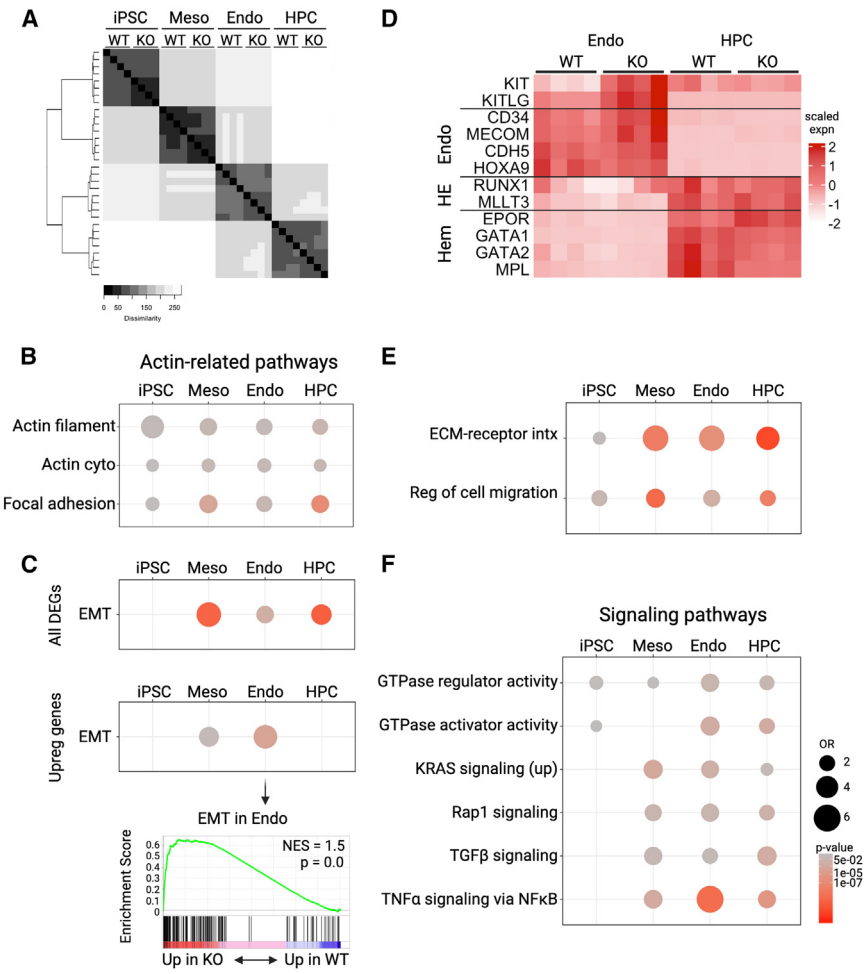

Figure 2. *TPM1*-deficient cultures show normal maturation with altered expression of genes and pathways that support cell state transitions (EMT/EHT) and HE formation

(A) Heatmap demonstrates similarity of isogenic CHOP14 WT and *TPM1KO* samples at the iPSC, mesoderm, endothelial, and HPC stages of development.

(B) Pathway analyses at the specified stages reveal changes in actin and focal adhesion pathways over the course of development. Bubble plots depict enrichment odds ratios (ORs), and color reflects statistical enrichment (*p* values) for the indicated pathways in *TPM1KO* vs. isogenic WT control cells.

(C) EMT-related gene expression is altered in *TPM1KO* cells at the mesoderm, endothelial, and HPC stages. EMT genes were specifically upregulated in *TPM1KO* endothelial cells. By gene set enrichment analysis, *TPM1KO* increases an EMT signature in endothelial cells. NES, normalized enrichment score.

(D) Select endothelial, HE, and hematopoietic (Hem) gene expression in WT and *TPM1KO* cells at the endothelial and HPC stages.

(E) Pathway analyses at the specified stages reveal changes in extracellular matrix-receptor interactions (ECM-receptor intx) and cell migration over the course of development. Bubble plots depict enrichment odds ratios (ORs), and color reflects statistical enrichment (*p* values) for the indicated pathways in *TPM1KO* vs. isogenic WT control cells.

(F) Pathway analyses at the specified stages reveal changes in signaling pathways over the course of development. Bubble plots depict enrichment odds ratios (ORs), and color reflects statistical enrichment (*p* values) for the indicated pathways in *TPM1KO* vs. isogenic WT control cells.

cells remain elusive, we also used intracellular RUNX1 expression to quantify HE cells in *TPM1KO* and isogenic control cultures (Cheng et al., 2023). These experiments revealed a ~2-fold change in HE cells among *TPM1KO* cultures, consistent with our limiting dilution experiments (Figures S2D and S2E).

We then performed colony assays to determine whether *TPM1KO* HPCs had any functional limitations or lineage bias. *TPM1KO* HPCs showed normal quantitative and qualitative production of primitive erythroid, myeloid, and megakaryocyte colonies (Pavani et al., 2024) (Figures 3C and S2F–S2I). These results complemented prior findings that showed normal function in *TPM1KO* megakaryocytes (Thom et al., 2020a) and showed that each *TPM1KO* HE cell retains normal HPC-producing capabilities. Thus, *TPM1* deficiency enhances total *in vitro* HPC output by increasing HE cell specification (Figure 3D).

TPM1 expression changes during *in vivo* HE specification and EMT/EHT

We then asked whether *TPM1* also regulated *in vivo* hematopoietic development. To assess *TPM1* expression in relevant cell types, we analyzed recently published single-cell RNA (scRNA) sequencing datasets of human and mouse hematopoietic cells (Calvanese et al., 2022; Zhu et al., 2020; Korsunsky et al., 2019). Among profiled human embryonic/fetal cells, high *TPM1* expression was observed in both stroma and epithelial subsets (Figure S2J). Lower *TPM1* expression was seen in other cell populations, including HE cells (Figure S2J). The diminished *TPM1* expression in HE and HPCs matched our *in vitro* data (Figure 1B), suggesting that *TPM1* expression is normally decreased during HE cell specification.

Interestingly, *TPM1* expression correlated with EMT/EHT progression in these datasets. By scoring each cell based on

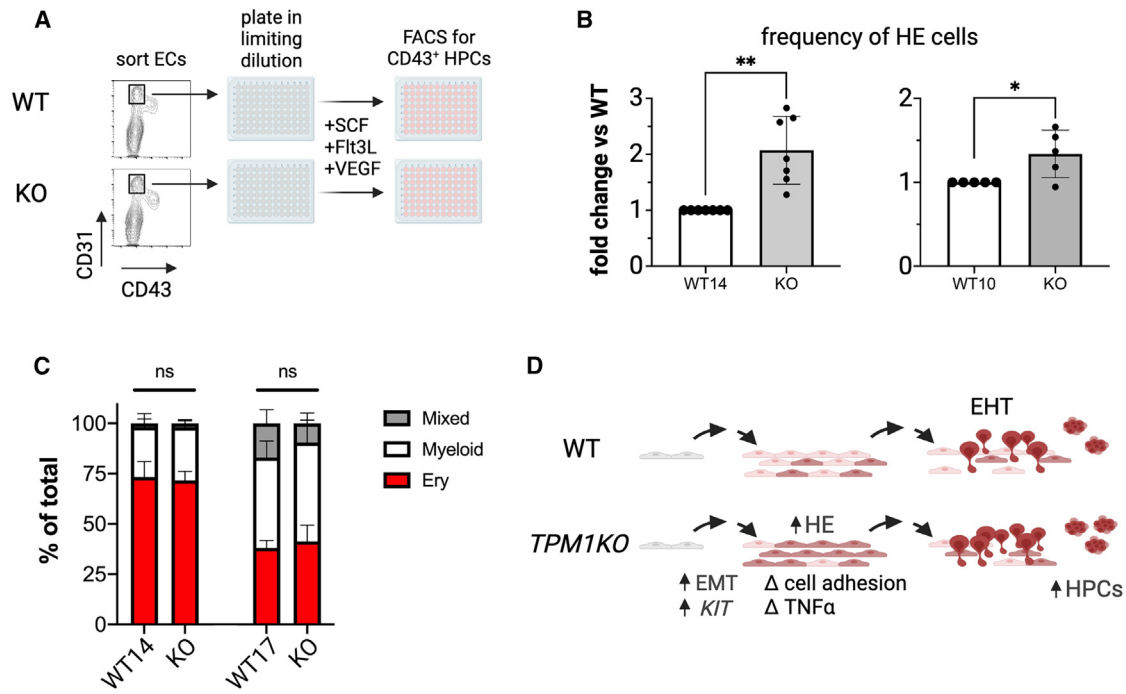

Figure 3. *TPM1* deficiency enhances HE cell specification during *in vitro* hematopoiesis

(A) To set up limiting dilution assays, $CD31^{+}CD43^{-}$ endothelial cells from *TPM1KO* and isogenic WT controls were sorted and plated in limiting dilution. After culturing in hematopoietic cytokines, the quantity of $CD43^{+}$ HPCs was quantified by fluorescence-activated cell sorting (FACS).

(B) The frequency of HE cells in *TPM1KO* vs. isogenic WT cultures were quantified and normalized to WT frequency in each experiment (n = 5–7 samples over 3–5 experiments). *p < 0.05, **p < 0.01.

(C) In colony formation assays, *TPM1KO* and isogenic WT controls produce similar numbers of erythroid, myeloid, and mixed colonies (n = 6–8 assays per group).

(D) During primitive *in vitro* hematopoiesis, *TPM1KO* alters EMT, signaling pathways, and gene expression to enhance yields of HE (brown) and functional HPCs.

its expression of established EMT-related genes (Andreatta and Carmona, 2021; Liberzon et al., 2015), higher EMT scores were noted to correlate with increased *TPM1* expression (Figure S2K). This observed increase in *TPM1* expression in cells undergoing EMT was also consistent with prior data from other cellular systems (Bakin et al., 2004, 2005; Dai and Gao, 2021; Pan et al., 2017; Wang et al., 2019). Targeted analysis of cells undergoing EHT revealed maximal *TPM1* expression in arterial endothelium (~pre-HE cells), with diminished expression in HE and more substantially reduced expression in HPCs following EHT completion (Figures S2K–S2M).

Tpm1 deficiency enhances murine HE specification in the E9.5 AGM region

To determine if our observations extended to the murine system, we analyzed scRNA sequencing data of murine embryonic cells undergoing hematopoiesis (Zhu et al., 2020). Similar to human development, murine $Runx1^{+}Cdh5^{+}$ HE cells form $Runx1^{+}$ HPCs that ultimately support lifelong hematopoiesis. These data largely excluded stromal and epithelial cells, which had the highest *TPM1* expression in human datasets. Consistent with human data, *Tpm1* expression increased in murine pre-hemogenic endothelium (pre-HE) and HE cells, with subsequent downregulation in HPCs (Figure 4A). Murine cells undergoing EHT also exhibited increased *Tpm1* expression (Figure S2K).

To analyze the impact of *Tpm1* on murine hematopoiesis, we obtained a *Tpm1* GeneTrap-Reporter mouse model ($Tpm1^{GT}$) (Bradley et al., 2012; Pettitt et al., 2009; Skarnes et al., 2011; White et al., 2013). This model contains an intronic splice acceptor site linked to a β-galactosidase reporter gene (LacZ) positioned to capture all *Tpm1* isoform transcripts (Figure S3A). Efficient capture of *Tpm1* transcripts by this construct was demonstrated by observing decreased Tpm1 protein in the peripheral blood of $Tpm1^{GT/+}$ mice and embryonic lethality in $Tpm1^{GT/GT}$ embryos (Figures S3B and S3C). The timing of lethality in $Tpm1^{GT/GT}$ embryos by E8.5–E9.5 was consistent with other *Tpm1* KO mouse models, which have reported severe

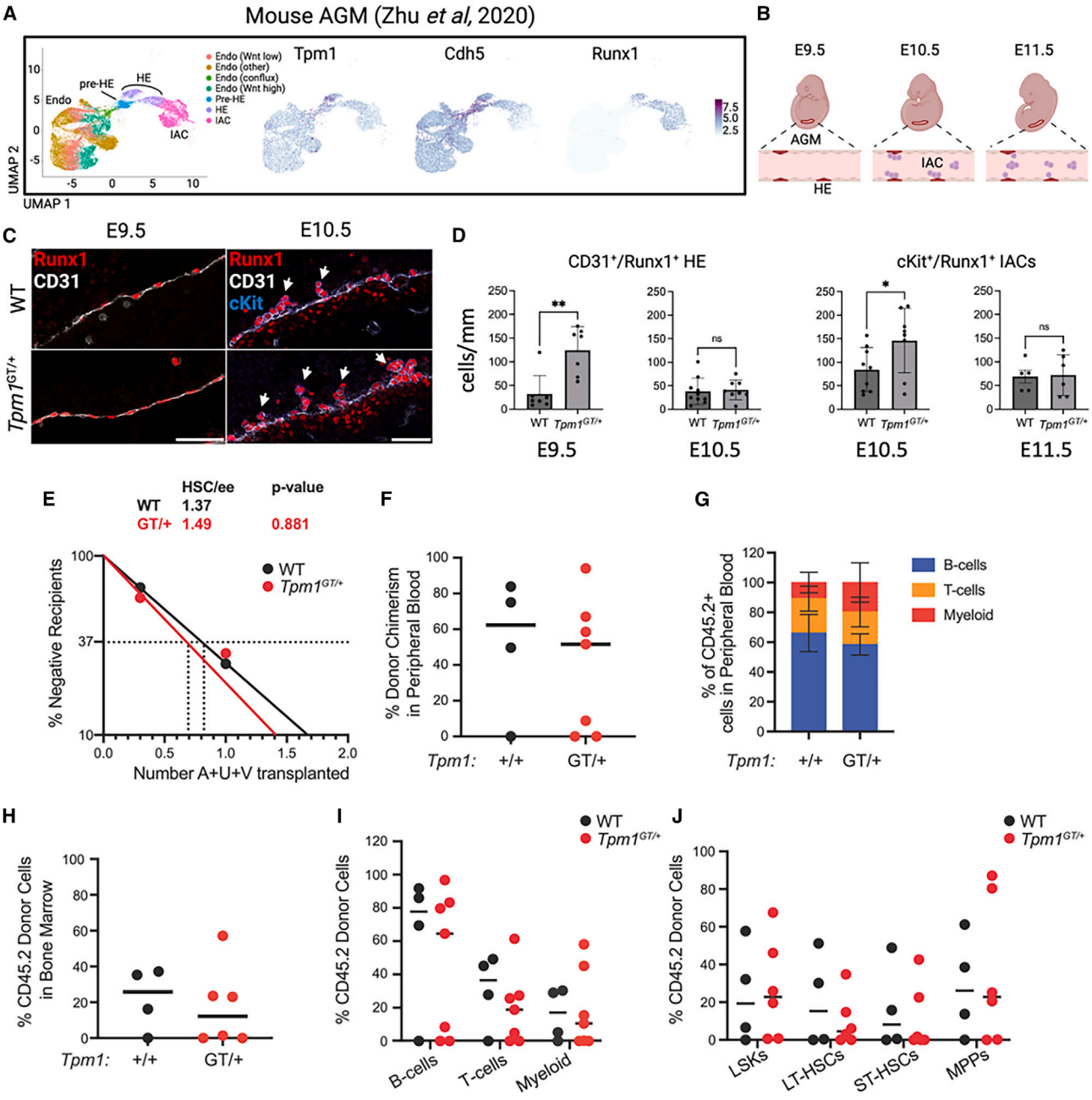

Figure 4. *Tpm1* regulates HE and HPC formation during *in vivo* murine hematopoiesis

(A) Single-cell sequencing analysis of murine cells derived from AGM, highlighting the EHT, with uniform manifold approximation and projection (UMAP) plots highlighting *Tpm1*, *Cdh5* (*VE-Cad*), and *Runx1* expression. Cell cluster labels are based on Zhu et al. (Zhu et al., 2020).

(B) During murine embryogenesis, CD31^{+}Runx1^{+} HE cells in the major caudal arteries emerge around E9.5. These HE cells form intra-aortic clusters (IACs) of cKit^{+}Runx1^{+} HPCs on E10.5–E11.5, which can be short-lived multipotent progenitor cells or engraftable hematopoietic stem cells that ultimately seed bone marrow to support lifelong hematopoiesis.

(C) Representative whole-mount staining of E9.5 and E10.5 aorta-gonad-mesonephros (AGM) from WT and *Tpm1*$^{GT/+}$ embryos. Arrows point to IACs. Scale bars, 50 μm.

(D) Quantifications of imaging studies show that heterozygous *Tpm1*$^{GT/+}$ mice have increased frequencies of HE cells at E9.5 and IAC cells at E10.5 compared to littermate controls. Visualizations were centered on the intersection of vitelline artery and dorsal aorta (n = 5–10 embryos per group). *p < 0.05, **p < 0.01 by two-tailed t test.

(legend continued on next page)

cardiac dysmorphology (Mckeown et al., 2014). However, *Tpm1*$^{GT/+}$ embryos did not show gross morphologic or endothelial abnormalities (Figure S3D). The presence of LacZ reporter expression in the E9.5 dorsal aortic endothelium of *Tpm1*$^{GT/+}$ embryos was also consistent with our expectations for *Tpm1* expression, based on protein expression during *in vitro* hematopoiesis (Figure S3E vs. Figure 1B).

To determine if the *Tpm1*^{GT} model showed enhanced HE cell specification, whole-mount imaging was performed to quantitate morphologically flat Runx1$^+$CD31$^+$ HE cells at E9.5 post-conception and round cKit$^+$Runx1$^+$ intra-aortic clusters (IACs) of HPCs at E10.5 (Tober et al., 2013; Zhu et al., 2020) (Figures 4B and 4C). *Tpm1*$^{GT/+}$ embryos showed enhanced quantities of HE cells at E9.5 and IACs at E10.5 (Figures 4C and 4D). Limiting dilution assays using E10.5 AGM cells confirmed a 43% increase in myeloid progenitor cell frequencies ($p = 0.03$ by chi-squared analysis) and no increase in lymphoid progenitor cell frequencies in *Tpm1*$^{GT/+}$ embryos vs. littermate controls (37% overall; B cell $p = 0.18$, T cell $p = 0.21$) (Figures S3F and S3G) (Zhu et al., 2020). Hematopoiesis in the E9.5 yolk sac was not significantly affected (Figures S3H and S3I). These findings suggested that *Tpm1* haploinsufficiency increased HE and myeloid HPC production in the AGM between E9.5–E10.5 *in vivo*.

We then interrogated a later wave of hematopoiesis in the AGM, which produces engraftable HSCs ~E10–E11.5 (Dignum et al., 2021; Müller et al., 1994). The number of HE cells was normal at E10.5, as were the quantities of IACs at E11.5 (Figure 4D) and HPCs in the E14.5 fetal liver (Figure S3J). Transplantation of E11.5 AGM tissue into irradiated recipients showed no significant differences in the number of HSCs between *Tpm1*$^{GT/+}$ embryos and WT littermate controls (Figures 4E–4J and S4). Taken together, these findings showed that *Tpm1* deficiency enhanced HE specification at E9.5 without augmenting engraftable HSC production.

DISCUSSION

This study reveals a novel role for *TPM1* in developmental hematopoiesis across species and hematopoietic ontogeny, from *in vitro* human primitive hematopoiesis to *in vivo* murine AGM hematopoiesis. The conserved role of *TPM1* may reflect the importance of actin regulation and actomyosin contractility across hematopoietic ontogeny (Lancino et al., 2018), despite differences in other supporting factors that vary (e.g., dependence on blood flow [Lucitti et al., 2007; Lundin et al., 2020]). *TPM1* downregulation normally occurs during HE specification in human cells, and *TPM1* deficiency is sufficient to augment the formation of HE and functional HPCs. Many studies have focused on transcription factors (e.g., *Runx1*) that drive hematopoiesis through "inside-out" mechanisms, i.e., transcriptional changes that promote altered morphology and cellular development (Gao et al., 2018; Ottersbach, 2019). *TPM1*-related mechanisms instead represent a distinct "'outside-in" paradigm wherein targeted perturbation of an actin regulatory molecule alters actin cytoskeletal dynamics and cell interactions to impact downstream transcriptional and/or developmental programs, including HE cell specification.

Mammalian cells can express >40 tropomyosin isoforms, and *TPM1* isoforms can have dramatically different biological effects (Gunning and Hardeman, 2017). Our findings indicate that the aggregated effect of *TPM1* gene products is to constrain, but not compromise, hematopoiesis. A limitation of this study is that all *in vitro* and *in vivo* models presented herein reflect coordinate depletion of all *TPM1* isoforms. While future studies are needed to conditionally

(E) Quantification of HSCs in E11.5 WT and *Tpm1*$^{GT/+}$ embryos by limiting dilution transplantation of 0.3 and 1.0 embryo equivalent (ee) cells from the AGM region, umbilical, and vitelline arteries (CD45.2) into CD45.1 adult recipients. Multi-lineage reconstitution was assessed as >1% donor myeloid (Mac1$^+$, Mac1$^+$Gr1$^+$), T cells (CD3$^+$) and B cells (CD19$^+$) in the peripheral blood 16 weeks post-transplantation. The number of HSCs was calculated using ELDA software. WT 1 ee $n = 4$, 0.3 ee $n = 6$; *Tpm1*$^{GT/+}$ 1 ee $n = 7$, 0.3 ee $n = 12$. $p = 0.88$.

(F) Percent donor (CD45.2$^+$) chimerism in peripheral blood of recipients at 16 weeks post-transplant, dose = 1 embryo equivalent. WT $n = 4$, *Tpm1*$^{GT/+}$ $n = 7$. t test, two-tailed, p value = 0.62.

(G) Percent of myeloid (Mac1$^+$, Mac1$^+$Gr1$^+$), T cells (CD3$^+$), and B cells (CD19$^+$) in donor cells (CD45.2$^+$) in the peripheral blood at 16 weeks post-transplant. Frequencies of lineage populations are only shown for recipients with multi-lineage chimerism (>1% CD45.2 contribution to each lineage). WT $n = 4$, *Tpm1*$^{GT/+}$ $n = 7$. There were no significant differences by two-way ANOVA with Sidak correction for multiple testing.

(H) Percent donor (CD45.2$^+$) chimerism in bone marrow 16 weeks post-transplant in recipients of 1ee of E11.5 AGMs from WT and *Tpm1*$^{GT/+}$. Donor WT $n = 4$, *Tpm1*$^{GT/+}$ $n = 6$; chimerism shown is from all live single cells in the bone marrow. No significant differences were identified by two-tailed t test.

(I) Percent donor (CD45.2$^+$) contribution to lineage cells (Mac1$^+$ and Mac1$^+$Gr1$^+$ myeloid, CD3$^+$ T cells, CD19$^+$ B cells) in the bone marrow. WT $n = 4$, *Tpm1*$^{GT/+}$ $n = 6$. No significant differences were identified by two-way ANOVA with Sidak correction for multiple testing.

(J) Percent donor (CD45.2$^+$) contribution to hematopoietic stem and progenitor cells in the bone marrow. Populations shown are LSK (Lin$^-$Sca-1$^+$kit$^+$), LT-HSCs (CD48$^-$CD150$^+$LSKs), ST-HSCs (CD48$^-$CD150$^-$LSKs), and MPPs (CD48$^+$CD150$^-$LSKs). WT $n = 4$, *Tpm1*$^{GT/+}$ $n = 6$. No significant differences were identified by two-way ANOVA with Sidak correction for multiple testing.

delete specific *TPM1* isoforms, high-molecular-weight *TPM1* isoforms (e.g., *TPM1.6/1.7*) seem most likely to directly constrain HE specification and/or EHT, given established effects in cell models (Bakin et al., 2004, 2005; Dai and Gao, 2021; Pan et al., 2017; Wang et al., 2019) and an increased presence of these isoforms in adherent cell types (Figure 1B). However, it has thus far been difficult to define functions for specific *TPM1* isoforms using overexpression studies during *in vitro* hematopoiesis (data not shown). Multiple isoforms may contribute independently to the regulatory effect of *TPM1* on normal hematopoiesis.

Effects observed herein may also have relevance for non-hematopoietic tissue development. Increased *TPM1* expression in stromal and epithelial cells undergoing EMT may indicate a more general regulatory role for *TPM1* during cell state transitions in embryonic cells (Figure S2K). This is consistent with previous studies that have also suggested links between TPM1 and EMT, although the role of TPM1 in promoting or inhibiting EMT progression has differed depending on cell or tissue context. Whereas concurrent *TPM1* and *TPM2* KO has a deleterious effect on ocular lens development (Shibata et al., 2021), *TPM1* deficiency seems to promote EMT in cancer models (Bakin et al., 2004, 2005; Dai and Gao, 2021; Pan et al., 2017; Wang et al., 2019). The hematopoietic system represents another example wherein *TPM1* deficiency positively impacts an EMT-like process.

In vitro-derived blood cells have recently been shown to support the production of clinical testing reagents (An et al., 2022) and cell therapeutics (An et al., 2018; Goldenson et al., 2022; Thom et al., 2020b), but blood cell yields remain inefficient. Factors influencing HE specification have been elusive but could be co-opted to enhance *in vitro* hematopoiesis. Our findings suggest that temporal modulation of *TPM1* may represent a novel strategy to increase formation of HE and certain blood cell types *in vitro*. The general cellular mechanisms by which *TPM1* regulates endothelial cell production during *in vitro* hematopoiesis may also facilitate derivation of other endothelial populations, including production of pulmonary endothelial cells to support cellular therapeutics development (Kolesnichenko et al., 2021; Wang et al., 2021).

In addition to defining a novel role for *TPM1* in hematopoiesis, our findings raise interesting questions about the regulation of different hematopoietic progenitor populations. Multiple waves of HE cells produce HPCs with different engraftment and differentiation potentials (Calvanese et al., 2022; Patel et al., 2022). Our studies triangulate the effects of *Tpm1* to E9.5 HE cell specification and the production of myeloid progenitors at ~E10.5 during murine embryogenesis (Dignum et al., 2021), without overt impact on engraftable HSC production (Figure 4). It is possible that *Tpm1* expression may impact the "arterial program" necessary for engraftable HSCs through direct or indirect impacts on HE cells (Dignum et al., 2021), with *Tpm1*-regulated actin-mediated cell contacts preventing premature escape from the AGM region. *TPM1* is indeed expressed in stromal and epithelial populations (Figures 1B and S2J), which could support HE cell interactions within perivascular niches that support hematopoiesis (Gonzalez Galofre et al., 2024).

Results of this study will inform targeted analyses to elucidate how *TPM1* regulates specific cell types and mechanisms. Our findings argue against an embryonic or fetal origin for previously identified links between polymorphisms in the *TPM1* gene locus and altered human blood traits (Chen et al., 2020; Vuckovic et al., 2020). Instead, *TPM1* seems likely to alter quantitative platelet and/or red blood cell traits by impacting blood cell formation and/or function in the postnatal environment. While we did not identify effects on E9.5 yolk sac hematopoiesis in the mouse embryo (Figure S3J), *TPM1* may impact yolk sac at earlier time points. Additionally, epistatic interactions between *TPM1* and TNF-α signaling modulation warrant future investigation. Broadly, the radical changes required to form HE, HPCs, and mature blood cells represent an exciting area of study for actin and tropomyosin biology.

EXPERIMENTAL PROCEDURES

Resource availability

Lead contact

Further information and requests for resources and reagents should be directed to and will be fulfilled by the lead contact Christopher S Thom, MD, PhD (thomc@chop.edu).

Materials availability

All iPSC lines and murine constructs are available upon request.

Data and code availability

All coding scripts are available on GitHub (https://github.com/thomchr/Tpm1HE) and by request. Primary RNA sequencing data were deposited at the Gene Expression Omnibus (GEO) under accession code GSE244112. All coding scripts and data are available by request. Public scRNA sequencing analyses were collected from GSE137117 (murine) and GSE162950 (human).

Stem cell generation and culture

WT control iPSC lines were obtained from the Children's Hospital of Philadelphia Pluripotent Stem Cell Core. *TPM1* KO cell lines were created using CRISPR-Cas9 (Maguire et al., 2022) and then validated (Thom et al., 2020a; Wilken et al., 2023). See supplemental information for culture details.

Primitive *in vitro* hematopoiesis

The primitive hematopoietic differentiation used in this study was previously described (Thom et al., 2020a; Wilken et al., 2023). See supplemental information for a full description of this protocol, including TNF-α modulation methods.

Western blots and flow cytometry

See supplemental information for methods and Table S3 for antibodies used.

Cell proliferation and cell-cycle analyses

CFSE and EdU staining were conducted according to the manufacturer's instructions (Thermo Fisher Scientific). See supplemental information for details.

Bulk RNA sequencing

Bulk RNA was isolated from cultured cells at indicated time points using a PureLink RNA micro kit (Invitrogen) according to the manufacturer's instructions. See supplemental information for library preparation and analysis methods.

Limiting dilution assay quantitation

Endothelial cells ($CD31^+$ or $CD34^+$) were isolated from primitive hematopoietic differentiations and sorted on a MoFlo Astrios (Beckman Coulter) into pre-treated 96-well tissue culture plates containing growth factor-reduced Matrigel. Cells were plated at 3–1,000 cells per well and cultured for 1 week in bFGF, SCF, Flt3L, and VEGF. Media were added every 2–3 days. After a week, adherent and non-adherent cells were harvested from each well, stained, and analyzed by flow cytometry. Wells containing at least 10 $CD43^+$ HPCs were deemed "positive" as having initially contained HE. For murine embryo limiting dilution assays, whole E10.5 embryos were dissociated and processed as described (Zhu et al., 2020). Progenitor cell frequencies were calculated using extreme limiting dilution analysis (ELDA) software (Hu and Smyth, 2009).

Colony-formation assays

Colony assays were performed according to the manufacturer's instructions with MegaCult-C or MethoCult H4435 enriched media (STEMCELL Technologies) using fresh or cryopreserved HPCs. See supplemental information for full details.

scRNA sequencing analysis

Single cell RNA sequencing data were acquired for human (Calvanese et al., 2022) or mouse (Zhu et al., 2020). See supplemental information for processing and analysis methods.

Mouse line derivation

Tpm1 GeneTrap-Reporter mouse embryos were obtained from the Wellcome Trust Sanger Institute Mouse Genetics Project (129-TPM1<tm1a(EUCOMM)Wtsi>/WtsiH) and backcrossed to C57Bl6/J mice (Jackson Labs). See supplemental information for full details. The Children's Hospital Institutional Animal Use and Care Committee approved all mouse studies.

Whole-mount embryo imaging

Whole-mount imaging was carried out as previously described (Tober et al., 2013; Schindelin et al., 2012). See supplemental information for details and Table S3 for antibodies used.

Yolk sac and fetal liver analyses

Freshly harvested E9.5 yolk sacs or E14.5 fetal livers were isolated, processed, and analyzed as described in supplemental information.

Bone marrow transplantation

B6.SJL-*Ptprc*^{a}*Pepc*^{b}/BoyCrCrl (CD45.1) were treated with a split dose of 900 cGy, 4 h apart. Each recipient received either 1 or 0.3 embryo equivalents (ee) of E11.5 AGMs from timed matings (CD45.2). AGMs were transplanted with 2.5×10^5 CD45.1/CD45.2 splenocytes by retro-orbital injection. Peripheral blood was taken at 4, 8, 12, and 16 weeks post-transplant, and bone marrow was analyzed at 16 weeks to assess donor chimerism in recipient mice. Antibodies used for these studies are listed in Table S3. HSC frequencies were determined by ELDA (Hu and Smyth, 2009).

Statistics and data plotting

Statistics and data were calculated and plotted using GraphPad Prism 9 or R (v4.2.2). Graphical schematics were generated using BioRender (www.BioRender.com).

SUPPLEMENTAL INFORMATION

Supplemental information can be found online at https://doi.org/10.1016/j.stemcr.2024.08.001.

ACKNOWLEDGMENTS

We thank the Children's Hospital of Philadelphia (CHOP) Flow Cytometry, Pluripotent Stem Cell, and Mouse Transgenic Cores for their assistance with this study. We thank Drs. Harry Ischiropoulos, Serena Raimo, and Ipsita Mohanty for their helpful guidance and assistance. We thank John Daniels, Nasir Riley, and the CHOP High Performance Computing Cluster support team for their help throughout this project. This study was funded by the National Institutes of Health (NICHD T32HD043021, NHLBI U24HL134763, and NHLBI K99HL56052 to C.S.T.; NHLBI U01HL134696 to S.T.C./D.L.F./P.G.; NHLBI R01HL091724 and R01HL163265 to N.A.S.), the Children's Hospital of Philadelphia Division of Neonatology (Fellows Research Award to C.S.T.), and a Children's Hospital of Philadelphia K-readiness Award (C.S.T.).

AUTHOR CONTRIBUTIONS

M.B.W., G.F., R.Q., L.B., J.T., C.N., G.P., V.T., J.A.M., A.G., N.O., P.G., S.T.C., N.A.S., D.L.F., and C.S.T. performed, analyzed, and/or interpreted cultured stem cell and/or mouse studies. J.G. and C.S.T. performed, analyzed, and interpreted computational experiments. C.S.T. wrote the paper and supervised the work. All authors edited and confirmed the final version of the manuscript.

DECLARATION OF INTERESTS

The authors declare no competing interests.

Received: October 9, 2023
Revised: July 29, 2024
Accepted: August 5, 2024
Published: August 29, 2024

REFERENCES

An, H.H., Poncz, M., and Chou, S.T. (2018). Induced Pluripotent Stem Cell-Derived Red Blood Cells, Megakaryocytes, and Platelets: Progress and Challenges. Curr. Stem Cell Rep. *4*, 310–317.

An, H.H., Gagne, A.L., Maguire, J.A., Pavani, G., Abdulmalik, O., Gadue, P., French, D.L., Westhoff, C.M., and Chou, S.T. (2022). The use of pluripotent stem cells to generate diagnostic tools for transfusion medicine. Blood *140*, 1723–1734.

Andreatta, M., and Carmona, S.J. (2021). UCell: Robust and scalable single-cell gene signature scoring. Comput. Struct. Biotechnol. J. *19*, 3796–3798. https://doi.org/10.1016/j.csbj.2021.06.043.

Bakin, A., Varga, A., Zheng, Q., and Safina, A. (2005). Epigenetic silencing of tropomyosin alters transforming growth factor beta control of cell invasion and metastasis. Breast Cancer Res. *7*, P4.15.

Bakin, A.V., Safina, A., Rinehart, C., Daroqui, C., Darbary, H., and Helfman, D.M. (2004). A Critical Role of Tropomyosins in TGF-Regulation of the Actin Cytoskeleton and Cell Motility in Epithelial Cells. Mol. Biol. Cell *15*, 4682–4694.

Bradley, A., Anastassiadis, K., Ayadi, A., Battey, J.F., Bell, C., Birling, M.C., Bottomley, J., Brown, S.D., Bürger, A., Bult, C.J., et al. (2012). The mammalian gene function resource: The International Knockout Mouse Consortium. Mamm. Genome *23*, 580–586.

Brayford, S., Bryce, N.S., Schevzov, G., Haynes, E.M., Bear, J.E., Hardeman, E.C., and Gunning, P.W. (2016). Tropomyosin promotes lamellipodial persistence by collaborating with Arp2/3 at the leading edge. Curr. Biol. *26*, 1312–1318.

Calvanese, V., Capellera-Garcia, S., Ma, F., Fares, I., Liebscher, S., Ng, E.S., Ekstrand, S., Aguadé-Gorgorió, J., Vavilina, A., Lefaudeux, D., et al. (2022). Mapping human haematopoietic stem cells from haemogenic endothelium to birth. Nature *604*, 534–540.

Canu, G., Athanasiadis, E., Grandy, R.A., Garcia-Bernardo, J., Strzelecka, P.M., Vallier, L., Ortmann, D., and Cvejic, A. (2020). Analysis of endothelial-to-haematopoietic transition at the single cell level identifies cell cycle regulation as a driver of differentiation. Genome Biol. *21*, 157.

Chen, X., and Oppenheim, J.J. (2016). Therapy: Paradoxical effects of targeting TNF signalling in the treatment of autoimmunity. Nat. Rev. Rheumatol. *12*, 625–626.

Chen, E.Y., Tan, C.M., Kou, Y., Duan, Q., Wang, Z., Meirelles, G.V., Clark, N.R., and Ma'ayan, A. (2013). Enrichr: interactive and collaborative HTML5 gene list enrichment analysis tool. BMC Bioinf. *14*, 128.

Chen, M.H., Raffield, L.M., Mousas, A., Sakaue, S., Huffman, J.E., Moscati, A., Trivedi, B., Jiang, T., Akbari, P., Vuckovic, D., et al. (2020). Trans-ethnic and Ancestry-Specific Blood-Cell Genetics in 746,667 Individuals from 5 Global Populations. Cell *182*, 1198–1213.e14.

Cheng, X., Barakat, R., Pavani, G., Usha, M.K., Calderon, R., Snella, E., Gorden, A., Zhang, Y., Gadue, P., French, D.L., et al. (2023). Nod1-dependent NF-kB activation initiates hematopoietic stem cell specification in response to small Rho GTPases. Nat. Commun. *14*, 7668.

Colin, A., Bonnemay, L., Gayrard, C., Gautier, J., and Gueroui, Z. (2016). Triggering signaling pathways using F-actin self-organization. Sci. Rep. *6*, 34657.

Coulombe, P., Cole, G., Fentiman, A., Parker, J.D.K., Yung, E., Bilenky, M., Degefie, L., Lac, P., Ling, M.Y.M., Tam, D., et al. (2023). Meis1 establishes the pre-hemogenic endothelial state prior to Runx1 expression. Nat. Commun. *14*, 4537.

Dai, Y., and Gao, X. (2021). Inhibition of cancer cell-derived exosomal microRNA-183 suppresses cell growth and metastasis in prostate cancer by upregulating TPM1. Cancer Cell Int. *21*, 145.

Dignum, T., Varnum-Finney, B., Srivatsan, S.R., Dozono, S., Waltner, O., Heck, A.M., Ishida, T., Nourigat-McKay, C., Jackson, D.L., Rafii, S., et al. (2021). Multipotent progenitors and hematopoietic stem cells arise independently from hemogenic endothelium in the mouse embryo. Cell Rep. *36*, 109675.

Dzierzak, E., and Speck, N.A. (2008). Of lineage and legacy: The development of mammalian hematopoietic stem cells. Nat. Immunol. *9*, 129–136.

Eilken, H.M., Nishikawa, S.I., and Schroeder, T. (2009). Continuous single-cell imaging of blood generation from haemogenic endothelium. Nature *457*, 896–900.

Espín-Palazón, R., Stachura, D.L., Campbell, C.A., García-Moreno, D., Del Cid, N., Kim, A.D., Candel, S., Meseguer, J., Mulero, V., and Traver, D. (2014). Proinflammatory signaling regulates hematopoietic stem cell emergence. Cell *159*, 1070–1085.

Gagat, M., Zielińska, W., Mikołajczyk, K., Zabrzyński, J., Krajewski, A., Klimaszewska-Wiśniewska, A., Grzanka, D., and Grzanka, A. (2021). CRISPR-Based Activation of Endogenous Expression of TPM1 Inhibits Inflammatory Response of Primary Human Coronary Artery Endothelial and Smooth Muscle Cells Induced by Recombinant Human Tumor Necrosis Factor α. Front. Cell Dev. Biol. *9*, 668032.

Gao, L., Tober, J., Gao, P., Chen, C., Tan, K., and Speck, N.A. (2018). RUNX1 and the endothelial origin of blood. Exp. Hematol. *68*, 2–9.

Gateva, G., Kremneva, E., Reindl, T., Kotila, T., Kogan, K., Gressin, L., Gunning, P.W., Manstein, D.J., Michelot, A., and Lappalainen, P. (2017). Tropomyosin Isoforms Specify Functionally Distinct Actin Filament Populations In Vitro. Curr. Biol. *27*, 705–713.

Goldenson, B.H., Hor, P., and Kaufman, D.S. (2022). iPSC-Derived Natural Killer Cell Therapies - Expansion and Targeting. Front. Immunol. *13*, 841107.

Goldie, L.C., Lucitti, J.L., Dickinson, M.E., and Hirschi, K.K. (2008). Cell signaling directing the formation and function of hemogenic endothelium during murine embryogenesis. Blood *112*, 3194–3204.

Gonzalez Galofre, Z.N., Kilpatrick, A.M., Marques, M., Sá da Bandeira, D., Ventura, T., Gomez Salazar, M., Bouilleau, L., Marc, Y., Barbosa, A.B., Rossi, F., et al. (2024). Runx1+ vascular smooth muscle cells are essential for hematopoietic stem and progenitor cell development *in vivo*. Nat. Commun. *15*, 1653.

Gritz, E., and Hirschi, K.K. (2016). Specification and function of hemogenic endothelium during embryogenesis. Cell. Mol. Life Sci. *73*, 1547–1567.

Gunning, P.W., and Hardeman, E.C. (2017). Tropomyosins. Curr. Biol. *27*, R8–R13.

Howell, E.D., Yzaguirre, A.D., Gao, P., Lis, R., He, B., Lakadamyali, M., Rafii, S., Tan, K., and Speck, N.A. (2021). Efficient hemogenic endothelial cell specification by RUNX1 is dependent on baseline chromatin accessibility of RUNX1-regulated TGFβ target genes. Genes Dev. *35*, 1475–1489.

Hu, Y., and Smyth, G.K. (2009). ELDA: Extreme limiting dilution analysis for comparing depleted and enriched populations in stem cell and other assays. J. Immunol. Methods *347*, 70–78.

Kalluri, R., and Weinberg, R.A. (2009). The basics of epithelial-mesenchymal transition. J. Clin. Invest. *119*, 1420–1428.

Kissa, K., and Herbomel, P. (2010). Blood stem cells emerge from aortic endothelium by a novel type of cell transition. Nature *464*, 112–115.

Kolesnichenko, O.A., Whitsett, J.A., Kalin, T.V., and Kalinichenko, V.V. (2021). Therapeutic potential of endothelial progenitor cells in pulmonary diseases. Am. J. Respir. Cell Mol. Biol. *65*, 473–488.

Korsunsky, I., Millard, N., Fan, J., Slowikowski, K., Zhang, F., Wei, K., Baglaenko, Y., Brenner, M., Loh, P.R., and Raychaudhuri, S. (2019). Fast, sensitive and accurate integration of single-cell data with Harmony. Nat. Methods *16*, 1289–1296.

Kubo, E., Hasanova, N., Fatma, N., Sasaki, H., and Singh, D.P. (2013). Elevated tropomyosin expression is associated with epithelial-mesenchymal transition of lens epithelial cells. J. Cell Mol. Med. *17*, 212–221.

Kucukural, A., Yukselen, O., Ozata, D.M., Moore, M.J., and Garber, M. (2019). DEBrowser: Interactive differential expression analysis and visualization tool for count data. BMC Genom. *20*, 6.

Kuleshov, M.V., Jones, M.R., Rouillard, A.D., Fernandez, N.F., Duan, Q., Wang, Z., Koplev, S., Jenkins, S.L., Jagodnik, K.M., Lachmann, A., et al. (2016). Enrichr: a comprehensive gene set enrichment analysis web server 2016 update. Nucleic Acids Res. *44*, W90–W97.

Lancino, M., Majello, S., Herbert, S., De Chaumont, F., Tinevez, J.Y., Olivo-Marin, J.C., Herbomel, P., and Schmidt, A. (2018). Anisotropic organization of circumferential actomyosin characterizes hematopoietic stem cells emergence in the zebrafish. Elife *7*, e37355.

Li, R., Zhang, J., Wang, Q., Cheng, M., and Lin, B. (2022). TPM1 mediates inflammation downstream of TREM2 via the PKA/CREB signaling pathway. J. Neuroinflammation *19*, 257.

Liberzon, A., Birger, C., Thorvaldsdóttir, H., Ghandi, M., Mesirov, J.P., and Tamayo, P. (2015). The Molecular Signatures Database Hallmark Gene Set Collection. Cell Syst. *1*, 417–425.

Lucitti, J.L., Jones, E.A.V., Huang, C., Chen, J., Fraser, S.E., and Dickinson, M.E. (2007). Vascular remodeling of the mouse yolk sac requires hemodynamic force. Development *134*, 3317–3326.

Lundin, V., Sugden, W.W., Theodore, L.N., Sousa, P.M., Han, A., Chou, S., Wrighton, P.J., Cox, A.G., Ingber, D.E., Goessling, W., et al. (2020). YAP Regulates Hematopoietic Stem Cell Formation in Response to the Biomechanical Forces of Blood Flow. Dev. Cell *52*, 446–460.e5.

Maguire, J.A., Gadue, P., and French, D.L. (2022). Highly Efficient CRISPR/Cas9-Mediated Genome Editing in Human Pluripotent Stem Cells. Curr. Protoc. *2*, e590.

Marcelo, K.L., Sills, T.M., Coskun, S., Vasavada, H., Sanglikar, S., Goldie, L.C., and Hirschi, K.K. (2013). Hemogenic endothelial cell specification requires c-Kit, notch signaling, and p27-mediated cell-cycle control. Dev. Cell *27*, 504–515.

Mckeown, C.R., Nowak, R.B., Gokhin, D.S., and Fowler, V.M. (2014). Tropomyosin is required for cardiac morphogenesis, myofibril assembly, and formation of adherens junctions in the developing mouse embryo. Dev. Dyn. *243*, 800–817.

Meiring, J.C.M., Bryce, N.S., Wang, Y., Taft, M.H., Manstein, D.J., Liu Lau, S., Stear, J., Hardeman, E.C., and Gunning, P.W. (2018). Co-polymers of Actin and Tropomyosin Account for a Major Fraction of the Human Actin Cytoskeleton. Curr. Biol. *28*, 2331–2337.e5.

Müller, A.M., Medvinsky, A., Strouboulis, J., Grosveld, F., and Dzierzak, E. (1994). Development of hematopoietic stem cell activity in the mouse embryo. Immunity *1*, 291–301.

O'Connell, J., Porter, J., Kroeplien, B., Norman, T., Rapecki, S., Davis, R., McMillan, D., Arakaki, T., Burgin, A., Fox Iii, D., et al. (2019). Small molecules that inhibit TNF signalling by stabilising an asymmetric form of the trimer. Nat. Commun. *10*, 5795.

Ottersbach, K. (2019). Endothelial-to-haematopoietic transition: An update on the process of making blood. Biochem. Soc. Trans. *47*, 591–601.

Pan, H., Gu, L., Liu, B., Li, Y., Wang, Y., Bai, X., Li, L., Wang, B., Peng, Q., Yao, Z., and Tang, Z. (2017). Tropomyosin-1 acts as a potential tumor suppressor in human oral squamous cell carcinoma. PLoS One *12*, e0168900.

Patel, S.H., Christodoulou, C., Weinreb, C., Yu, Q., da Rocha, E.L., Pepe-Mooney, B.J., Bowling, S., Li, L., Osorio, F.G., Daley, G.Q., and Camargo, F.D. (2022). Lifelong multilineage contribution by embryonic-born blood progenitors. Nature *606*, 747–753.

Pavani, G., Klein, J.G., Nations, C.C., Sussman, J.H., Tan, K., An, H.H., Abdulmalik, O., Thom, C.S., Gearhart, P.A., Willett, C.M., et al. (2024). Modeling primitive and definitive erythropoiesis with induced pluripotent stem cells. Blood Adv. *8*, 1449–1463.

Pettitt, S.J., Liang, Q., Rairdan, X.Y., Moran, J.L., Prosser, H.M., Beier, D.R., Lloyd, K.C., Bradley, A., and Skarnes, W.C. (2009). Agouti C57BL/6N embryonic stem cells for mouse genetic resources. Nat. Methods *6*, 493–495.

Saxena, S., Rönn, R.E., Guibentif, C., Moraghebi, R., and Woods, N.B. (2016). Cyclic AMP Signaling through Epac Axis Modulates Human Hemogenic Endothelium and Enhances Hematopoietic Cell Generation. Stem Cell Rep. *6*, 692–703.

Schevzov, G., Whittaker, S.P., Fath, T., Lin, J.J., and Gunning, P.W. (2011). Tropomyosin isoforms and reagents. BioArchitecture *1*, 135–164.

Schindelin, J., Arganda-Carreras, I., Frise, E., Kaynig, V., Longair, M., Pietzsch, T., Preibisch, S., Rueden, C., Saalfeld, S., Schmid, B., et al. (2012). Fiji: an open-source platform for biological-image analysis. Nat. Methods *9*, 676–682.

Shibata, T., Ikawa, M., Sakasai, R., Ishigaki, Y., Kiyokawa, E., Iwabuchi, K., Singh, D.P., Sasaki, H., and Kubo, E. (2021). Lens-specific Conditional Knockout of Tropomyosin 1 Gene in Mice Causes Abnormal Fiber Differentiation and Lens Opacity.

Skarnes, W.C., Rosen, B., West, A.P., Koutsourakis, M., Bushell, W., Iyer, V., Mujica, A.O., Thomas, M., Harrow, J., Cox, T., et al. (2011). A conditional knockout resource for the genome-wide study of mouse gene function. Nature *474*, 337–342.

Thom, C.S., Jobaliya, C.D., Lorenz, K., Maguire, J.A., Gagne, A., Gadue, P., French, D.L., and Voight, B.F. (2020a). Tropomyosin 1 genetically constrains *in vitro* hematopoiesis. BMC Biol. *18*, 52.

Thom, C.S., Chou, S.T., and French, D.L. (2020b). Mechanistic and Translational Advances Using iPSC-Derived Blood Cells. J. Exp. Pathol. *1*, 36–44. https://doi.org/10.33696/pathology.1.010.

Tober, J., Yzaguirre, A.D., Piwarzyk, E., and Speck, N.A. (2013). Distinct temporal requirements for Runx1 in hematopoietic progenitors and stem cells. Development *140*, 3765–3776.

Vuckovic, D., Bao, E.L., Akbari, P., Lareau, C.A., Mousas, A., Jiang, T., Chen, M.H., Raffield, L.M., Tardaguila, M., Huffman, J.E., et al. (2020). The Polygenic and Monogenic Basis of Blood Traits and Diseases. Cell *182*, 1214–1231.e11.

Wang, G., Wen, B., Ren, X., Li, E., Zhang, Y., Guo, M., Xu, Y., Whitsett, J.A., Kalin, T.V., and Kalinichenko, V.V. (2021). Generation of pulmonary endothelial progenitor cells for cell-based therapy using interspecies mouse-rat chimeras. Am. J. Respir. Crit. Care Med. *204*, 326–338.

Wang, J., Tang, C., Yang, C., Zheng, Q., and Hou, Y. (2019). Tropomyosin-1 functions as a tumor suppressor with respect to cell proliferation, angiogenesis and metastasis in renal cell carcinoma. J. Cancer *10*, 2220–2228.

White, J.K., Gerdin, A.K., Karp, N.A., Ryder, E., Buljan, M., Bussell, J.N., Salisbury, J., Clare, S., Ingham, N.J., Podrini, C., et al. (2013). Genome-wide generation and systematic phenotyping of knockout mice reveals new roles for many genes. Cell *154*, 452–464.

Wilken, M.B., Maguire, J.A., Dungan, L.V., Gagne, A., Osorio-Quintero, C., Waxman, E.A., Chou, S.T., Gadue, P., French, D.L., and Thom, C.S. (2023). Generation of a human Tropomyosin 1 knockout iPSC line. Stem Cell Res. *71*, 103161.

Xie, Z., Bailey, A., Kuleshov, M.V., Clarke, D.J.B., Evangelista, J.E., Jenkins, S.L., Lachmann, A., Wojciechowicz, M.L., Kropiwnicki, E., Jagodnik, K.M., et al. (2021). Gene Set Knowledge Discovery with Enrichr. Curr. Protoc. *1*, e90.

Zhu, Q., Gao, P., Tober, J., Bennett, L., Chen, C., Uzun, Y., Li, Y., Howell, E.D., Mumau, M., Yu, W., et al. (2020). Developmental trajectory of prehematopoietic stem cell formation from endothelium. Blood *136*, 845–856.